Charles G. Brown Brigham Young University 459 CB, Provo, UT 84602

801-378-4884, FAX: 801-378-6586, e-mail: browncg@ee.byu.edu

Abstract—Traditional satellite scatterometer wind retrieval algorithms consist of point-wise wind estimation and point-wise ambiguity removal. Point-wise estimation yields multiple estimates, or ambiguities, for the near-surface ocean wind in each scatterometer resolution element, requiring subsequent ambiguity removal. Even though some point-wise ambiguity removal techniques achieve a high skill, they are still subject to error and usually rely on numerical model analysis fields.

An alternative to point-wise wind retrieval, one that does not rely on numerical model analysis fields, is field-wise or model-based retrieval. This paper presents an automated field-wise retrieval algorithm. The algorithm is tested on data obtained from the NASA Scatterometer (NSCAT), and results indicate that field-wise retrieval provides a reliable means of performing wind retrieval based on scatterometer measurements alone.

INTRODUCTION

Satellite scatterometer wind retrieval is the process of determining the near-surface ocean wind from scatterometer measurements. Traditional wind retrieval consists of point-wise wind estimation followed by point-wise ambiguity removal. While current point-wise estimation algorithms are reliable, the subsequent point-wise ambiguity removal schemes are subject to error, even though some achieve fairly high skill. Further, the most successful ambiguity removal techniques require outside information, such as numerical model analysis fields. This report investigates field-wise wind retrieval, an alternative to the traditional scheme. Field-wise retrieval does not utilize numerical weather prediction winds but relies only on scatterometer measurements.

FIELD-WISE WIND RETRIEVAL

Field-wise wind retrieval consists of field-wise estimation and field-wise ambiguity removal (Fig. 1), which determine a unique wind estimate given a swath of scatterometer measurements. Field-wise estimation determines the wind field for many resolution elements at once using a wind field model. The task of field-wise estimation is to determine op-

timal sets of model parameters, denoted by the column vector $\hat{\mathbf{X}}$, from scatterometer backscatter measurements over a rectangular region of the ocean's surface. The model-based wind field is the matrix product $\hat{\mathbf{W}} = F\hat{\mathbf{X}}$, where $\hat{\mathbf{W}}$ is a column vector containing the rectangular components of the wind in the region. The matrix F is the wind field model [Long, 1993].

The model parameters are estimated by locating all the local minima of the maximum likelihood objective function

$$J(\hat{\mathbf{W}} = F\hat{\mathbf{X}}) = -\sum_{n=1}^{N} \sum_{k=1}^{L_n} \ln p(z_n(k) \mid \hat{\mathbf{X}})$$
 (1)

with

$$p(z_n(k) \mid \hat{\mathbf{X}}) = \frac{1}{\sqrt{2\pi}} \frac{1}{\sqrt{\operatorname{Var}[z_n(k)]}} \cdot \exp\left\{-\frac{1}{2} \left[z_n(k) - \sigma_n^0(k)\right]^2 / \operatorname{Var}\left[z_n(k)\right]\right\}, \quad (2)$$

and $\sigma_n^0(k) = \mathcal{M}\{(u_n, v_n), k\}$. \mathcal{M} represents the geophysical model function that relates (u_n, v_n) , the vector wind in cell n, to the true value of $\sigma_n^0(k)$, which is the noiseless radar backscatter measurement that would be observed for the vector wind (u_n, v_n) . N is the number of resolution elements in the region of interest in the measurement swath, and n is the index of a particular element. L_n is the number of measurements in cell n. The k^{th} measurement in cell n is denoted $z_n(k)$, and $p(z_n(k) \mid \hat{\mathbf{X}})$ is the likelihood of observing $z_n(k)$ given that $\hat{\mathbf{W}} = F\hat{\mathbf{X}}$ is the true wind [Long, 1993].

As in the point-wise scheme, field-wise estimation produces multiple solutions (ambiguities). However, since the ambiguities are fields of vectors rather than individual vectors, adjacent solutions can be made to overlap, and continuity considerations can be invoked to greatly simplify ambiguity removal.

ALGORITHM

The field-wise retrieval algorithm used in this paper is diagrammed in Fig. 2. The first step in the algorithm locates the multiple solutions through fieldwise estimation, which is accomplished by two methods: a simple multistart algorithm and an algorithm

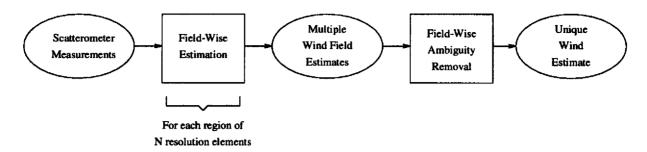


Figure 1: Field-wise wind retrieval is one possible alternative to the traditional retrieval method. A field-wise wind retrieval algorithm consists of field-wise estimation and field-wise ambiguity removal.

that utilizes median filter outputs. Both methods are described below. The resulting solutions are then ranked, and the highest ranked solutions are pieced together. Discontinuities in the estimates are removed by replacing poorly fitting solutions with lower-ranked solutions that preserve continuity from one overlapping region to another.

The field-wise estimation is performed on individual square regions whose sides are twelve 50km resolution elements long, corresponding to the low resolution cross-track width of the NASA Scatterometer (NSCAT) [Naderi et al., 1991]. Each NSCAT swath is divided into such regions overlapping by 50%. The first field-wise estimation algorithm uses a simple multi-start global optimization technique to identify multiple estimates. In the first stage of the algorithm, 50 model parameter sets for a 12 parameter Karhunen-Loeve (KL) model [Brown et al., 1997] are randomly chosen, and the field-wise objective function J is locally optimized using each model parameter set as an initial value. Next, the negative of each of the resulting estimates initializes local optimizations of J.

The second field-wise estimation algorithm takes advantage of ambiguity removal performed by the median filter [Naderi et al., 1991] initialized with point-wise ambiguities. The median filter produces two estimates, one when it is initialized with the first-ranked point-wise ambiguities and another when it is initialized with the second-ranked point-wise ambiguities. A 40 parameter KL model is fit to both outputs of the median filter. Each of the model fits initializes a local optimization of J. Finally, the closest point-wise ambiguity field is constructed for each optimized field and a 22 parameter KL model is fit to the closest ambiguity fields. These fits and the estimates from the first algorithm are pooled into a single collection of solutions.

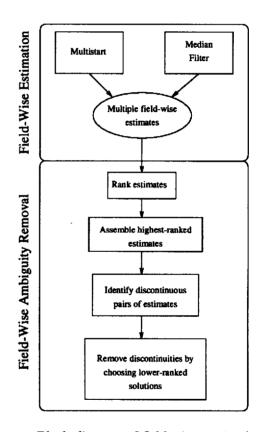


Figure 2: Block diagram of field-wise retrieval algorithm used in this paper

In order to rank the likelihood of each solution, the corresponding field of closest point-wise ambiguities is constructed for each of the multiple solutions. Each of the estimates is assigned a statistical ranking based on the sum of all the point-wise likelihood values in their corresponding closest-ambiguity fields.

Finally, field-wise ambiguity removal is performed by assembling the highest ranked solutions. This simple process yields remarkably good results, since the highest ranked field-wise estimate is the closest estimate (with only slight differences due to modeling error) to the true wind a much higher percentage of the time than the first-ranked point-wise ambiguity is the closest point-wise estimate to the true wind. In other words, the first field-wise ambiguity skill is dramatically higher than the first pointwise ambiguity skill. Thus, ambiguity removal can be performed simply by assembling the first ranked field-wise ambiguities, invoking continuity considerations to identify where a particular highest ranked solution does not fit and using lower-ranked solutions where needed. Areas where all combinations of possible solutions exhibit discontinuities are flagged as problematic, and the highest ranked solutions are retained as the selected estimates.

A simple justification of the observation that the first field-wise ambiguity skill is substantially higher than the first point-wise ambiguity skill may be obtained from the following analysis. Several simplifying assumptions are made: first, that modeling error is sufficiently low so that at least one of the closest ambiguity fields (to the multiple solutions) is the closest point-wise ambiguity field to the true wind, and second that the point-wise first ambiguity skill is approximately constant over any given region.

Under these assumptions, the probability that the closest ambiguity field to the first ranked field-wise estimate is the ambiguity field closest to the true wind (the first field-wise ambiguity skill) may be expressed in terms of the binomial distribution:

$$P(N,\theta) = \sum_{x=\lfloor \frac{N}{2} \rfloor + 1}^{N} {N \choose x} \theta^{x} (1-\theta)^{N-x},$$
 (3)

where N is the number of cells in the region and θ is the first point-wise ambiguity skill. Since θ is close to 0.5 and N is large, the normal approximation of the binomial distribution [Freund, 1992] gives

$$P(N,\theta) \approx \int_{\underbrace{\left(\left\lfloor \frac{N}{2}\right\rfloor + 1 - 0.5\right) - N\theta}_{\sqrt{N\theta}(1-\theta)}}^{\underbrace{\left(\left\lfloor \frac{N}{2}\right\rfloor + 1 - 0.5\right) - N\theta}_{\sqrt{N\theta}(1-\theta)}} \frac{1}{\sqrt{2\pi}} \exp^{-\frac{1}{2}\tau^2} d\tau, \tag{4}$$

where the ∓ 0.5 terms are continuity corrections. Since the integrand in equation (4) has a negligibly small value beyond the upper limit, a further simplification may be made:

$$P(N,\theta) \approx \lim_{\tau_2 \to \infty} \int_{\tau_1}^{\tau_2} \exp^{-\frac{1}{2}\tau^2} d\tau,$$
 (5)

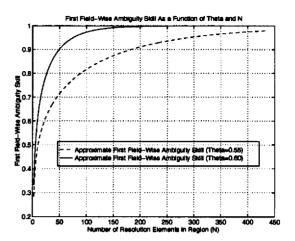


Figure 3: This figure is a graph of field-wise ambiguity skill for two values of the first point-wise ambiguity skill, θ , and over a range of even values of N. Field-wise estimates display high first ambiguity skill, and the skill tends to increase with N.

with
$$au_1 = rac{\left(\left\lfloor rac{N}{2}
ight
floor + 0.5
ight) - N heta}{\sqrt{N heta(1- heta)}}.$$

N is the number of cells in the region and θ is the first point-wise ambiguity skill. Figure 3 is a graph of the above equation for two values of θ and over a range of even values of N. It is clear that the first field-wise ambiguity skill is dramatically higher than that of the first-ranked point-wise ambiguity. Further, the first field-wise ambiguity skill tends to increase with N.

RESULTS

The algorithm described in the previous section was tested on a small set of NSCAT data, selected so that the JPL ambiguity removal product was subjectively considered to be reliable. The test set represented a range of wind features, such as uniform winds, fronts, cyclones, and low wind speed regions. The JPL product is derived from a median filter initialized using model analysis winds. The field-wise algorithm yields consistent results comparable to the JPL product, except in isolated regions. Many of the erroneous regions, however, are automatically flagged as problematic by the algorithm, and it is expected that further modifications will eliminate the unflagged regions. Comparison of the results to those of obtained from the median filter without model analysis winds suggests that the algorithm is clearly more accurate.

An example of the output of the field-wise retrieval algorithm is given in Fig. 4. In this section of the ascending NSCAT revolution 2456, the median filter without numerical model wind initialization (Fig. 5) suffers from severe ambiguity removal failures, while the field-wise output closely matches the JPL product (Fig. 6).

REFERENCES

- [Brown et al., 1997] Brown, C. G., P. E. Johnson, S. L. Richards, and D. G. Long, "Wind Field Models and Model Order Selection for Wind Estimation." In IGARSS, vol. 4, pp. 1847–1849, 1997.
- [Freund, 1992] Freund, J. E., Mathematical Statistics. Prentice-Hall, Englewood Cliffs, New Jersey, 5th edn., 1992.
- [Long, 1993] Long, D. G., "Wind Field Model-Based Estimation of Seasat Scatterometer Winds." Journal of Geophysical Research, vol. 98, no. C8, pp. 14651–14668, 1993.
- [Naderi et al., 1991] Naderi, F. M., M. H. Freilich, and D. G. Long, "Spaceborne Radar Measurement of Wind Velocity Over the Ocean—An Overview of the NSCAT Scatterometer System." Proceedings of the IEEE, vol. 79, no. 6, pp. 850– 866, 1991.

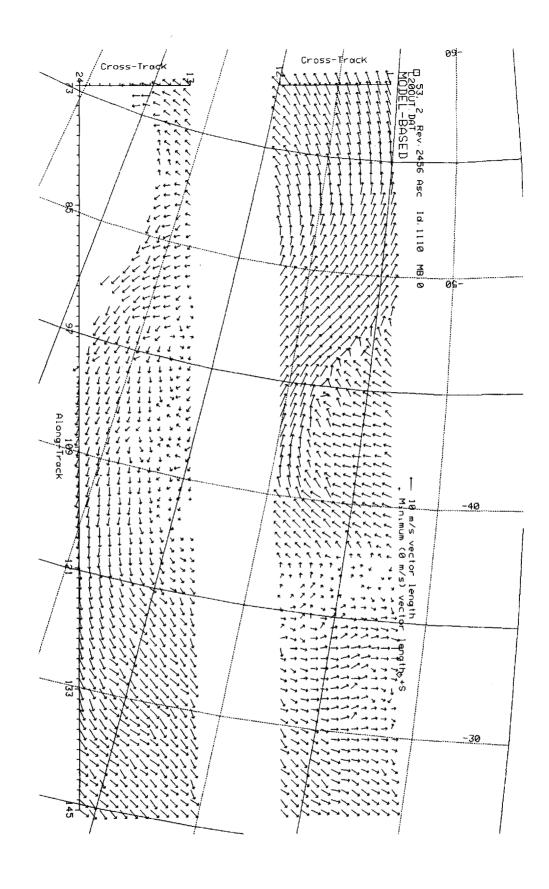


Figure 4: Plot of closest point-wise ambiguities to output of field-wise wind retrieval algorithm for a portion of ascending NSCAT revolution 2456

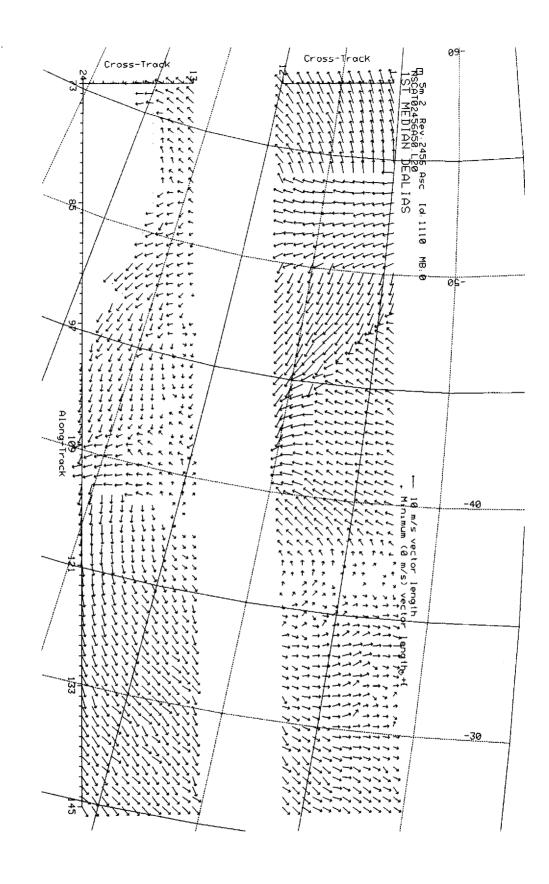


Figure 5: Plot of output of median filter initialized with first-ranked point-wise ambiguities for a portion of ascending NSCAT revolution 2456

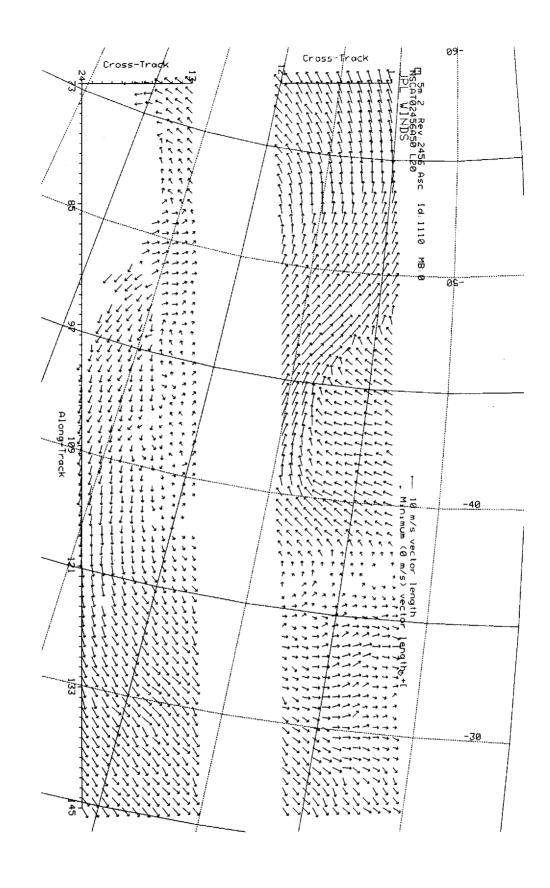


Figure 6: Plot of JPL ambiguity removal product for a portion of ascending NSCAT revolution 2456